

# Supplementary Materials: The Influence of the Mixed DPC:SDS Micelle on the Structure and Oligomerization Process of the Human Cystatin C

Przemyslaw Jurczak <sup>1,\*</sup> , Emilia Sikorska <sup>1</sup> , Paulina Czaplewska <sup>2</sup> , Sylwia Rodziewicz-Motowidlo <sup>1</sup> , Igor Zhukov <sup>3,4,\*</sup>  and Aneta Szymanska <sup>1,\*</sup> 

## Supporting information

Table S1: The values of critical micelle concentrations in PBS buffer, at 22°C and 37°C, for the surfactants used in this study<sup>1</sup>

surfactant	CMC
dodecylphosphocholine (DPC)	1.36 mM (22°C) 1.39 mM (37°C)
sodium dodecyl sulfate (SDS)	1.1 mM (22°C) 1.27 mM (37°C)
DPC:SDS 5:1	0.65 mM and 1.18 mM (22°C) 0.74 mM (37°C)

<sup>1</sup>Sikorska, E. et al. Thermodynamics, size, and dynamics of zwitterionic dodecylphosphocholine and anionic sodium dodecyl sulfate mixed micelles *J. Therm. Anal. Calorim.* **2016**, *123*, 511–523.

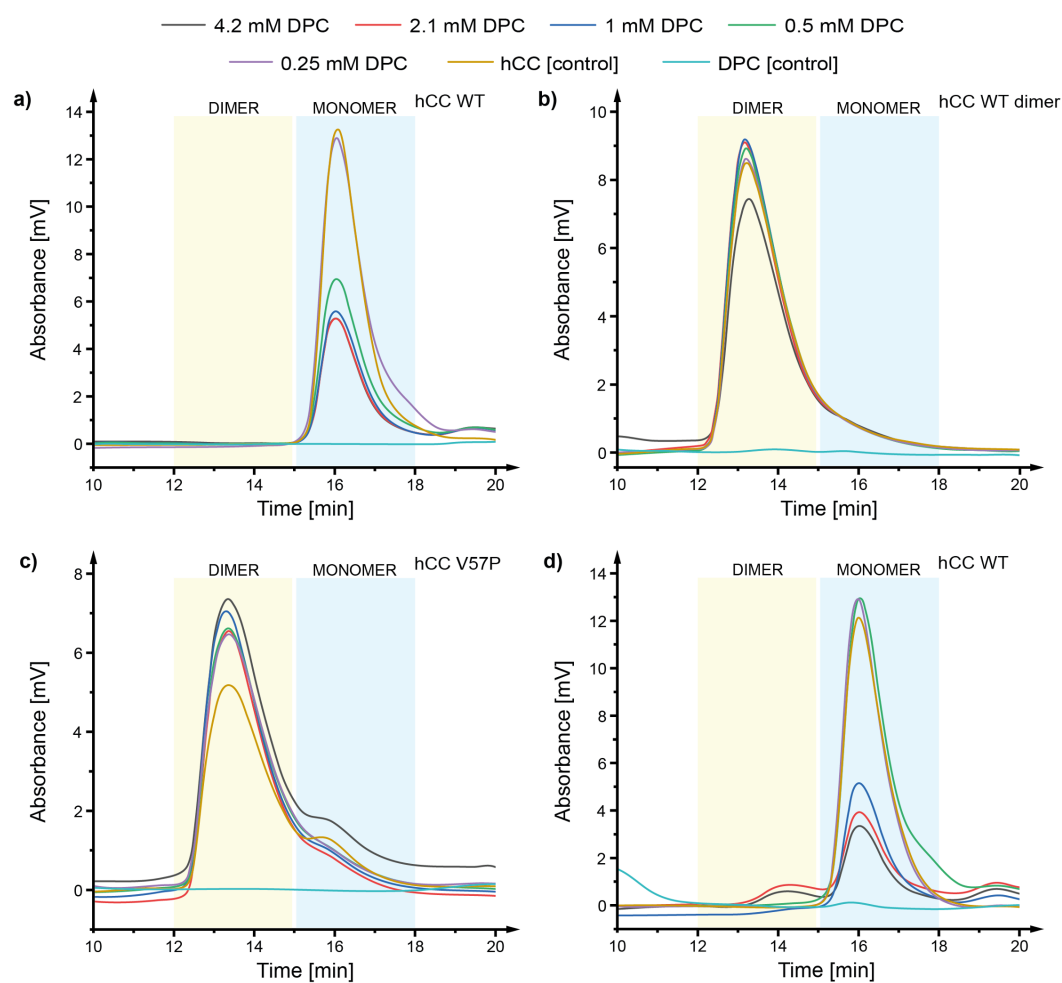


**Figure S1.** Chromatograms visualizing the separation of (a) *hCC* WT monomer, (b) WT dimer, and (c) V57P using the gel filtration chromatography after incubation for 24 h in the DPC solution at 22°C and (d) *hCC* WT monomer after incubation for 24 h in the DPC solution at 37°C (b); dimer retention time - ca. 13.5 min (yellow box), monomer retention time - ca. 16 min (blue box).

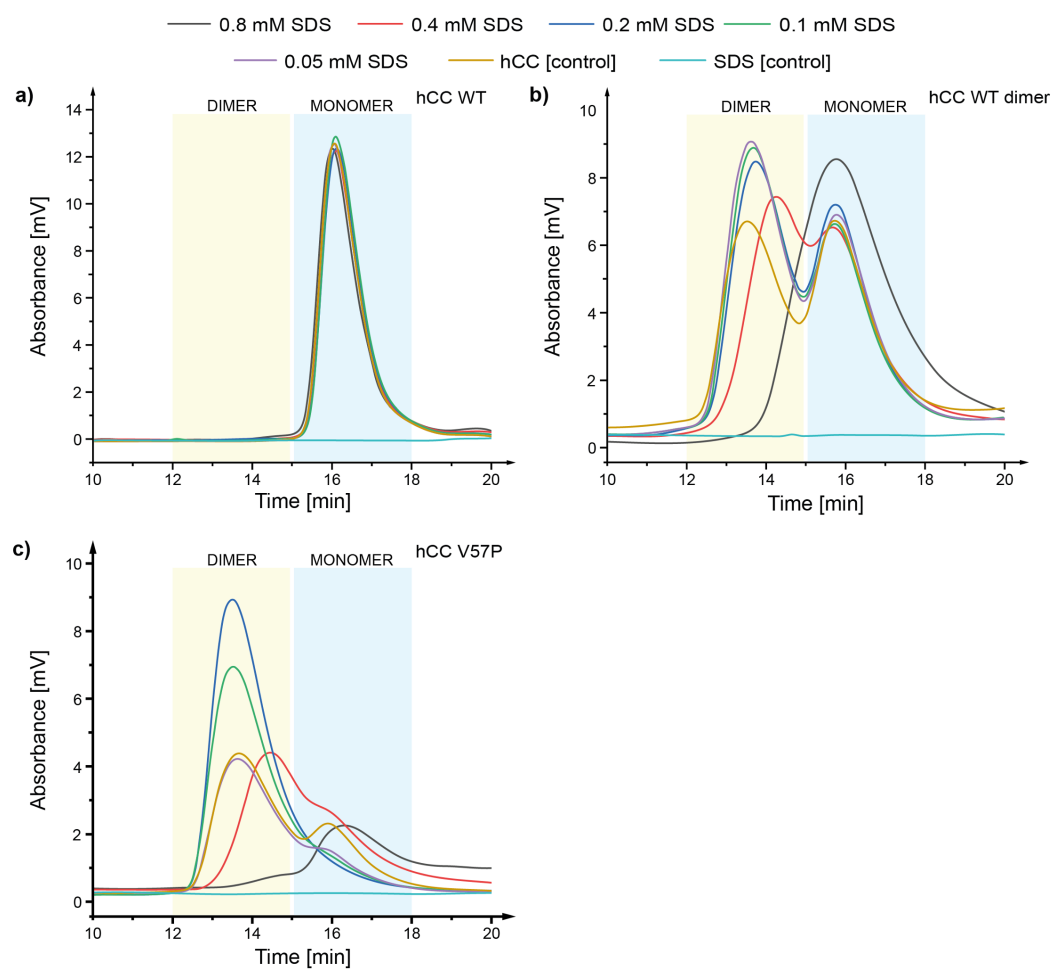


**Figure S2.** Chromatograms visualizing the separation of (a) *hCC* WT monomer, (b) *hCC* WT dimer and (c) *hCC* V57P using the gel filtration chromatography after incubation at 22°C for 24 h in the SDS solutions.

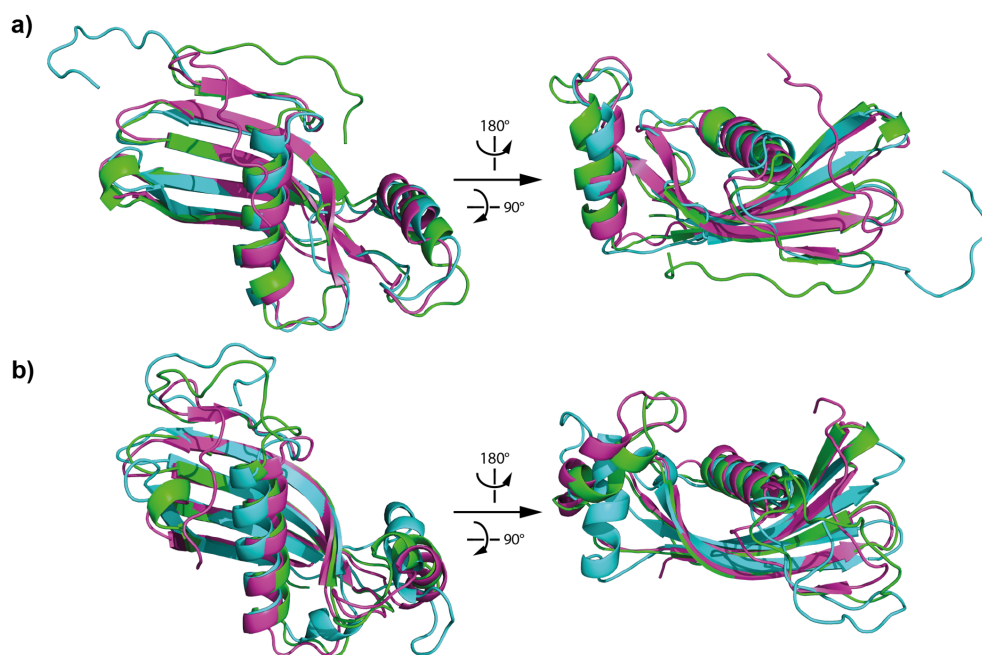


**Figure S3.** The structure of *hCC* V57G (a) before and (b) after 80 ns of MD simulation of *hCC*-DPC:SDS mixed micelle interaction; dynamics performed for three NMR structures differing mostly in the positioning of N-terminal part of the protein; NMR structure states: V57G-1 (green), V57G-2 (cyan), V57G-3 (magenta).



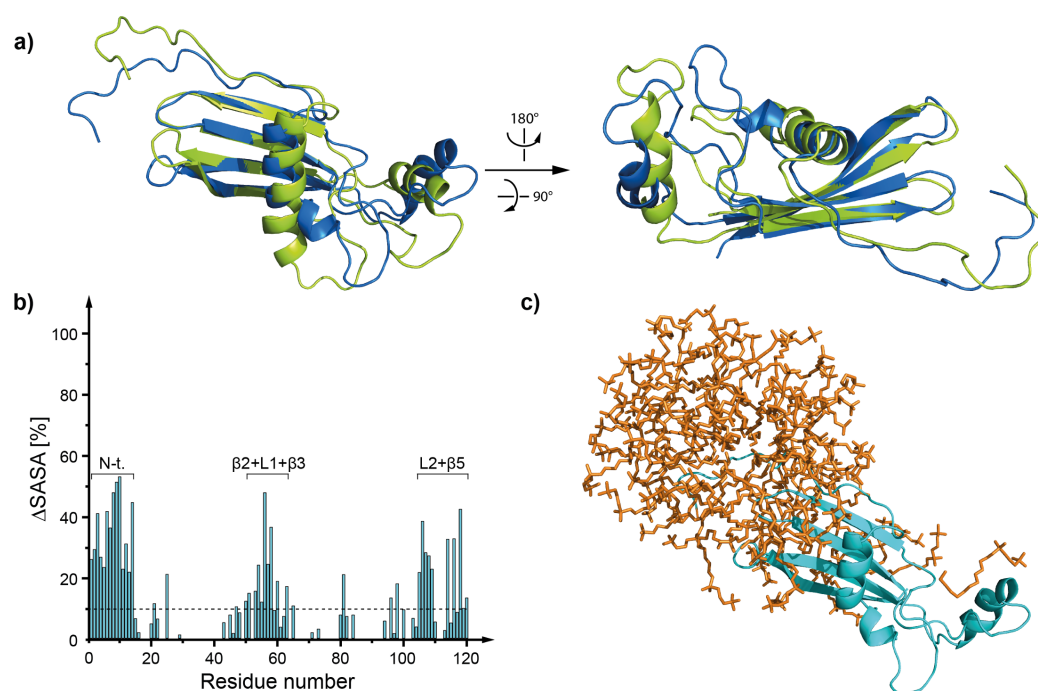


**Figure S5.** (a) The structure of *hCC* WT (*hCC*-2) monomer before (green) and after (blue) 80 ns of MD simulation of *hCC*-DPC:SDS mixed micelle interaction; (b) histogram visualizing the percentage of the decrease of solvent accessible surface occurring as a consequence of the interaction between *hCC* V57G monomer and DPC:SDS mixed micelle; (c) a model of *hCC* WT monomer protein interacting with the DPC:SDS mixed micelle, corresponding to the histogram (structure after 80 ns of MD); ΔSAS calculated as a difference between the SAS for the protein model without the micelle and protein model surrounded by the micelle.

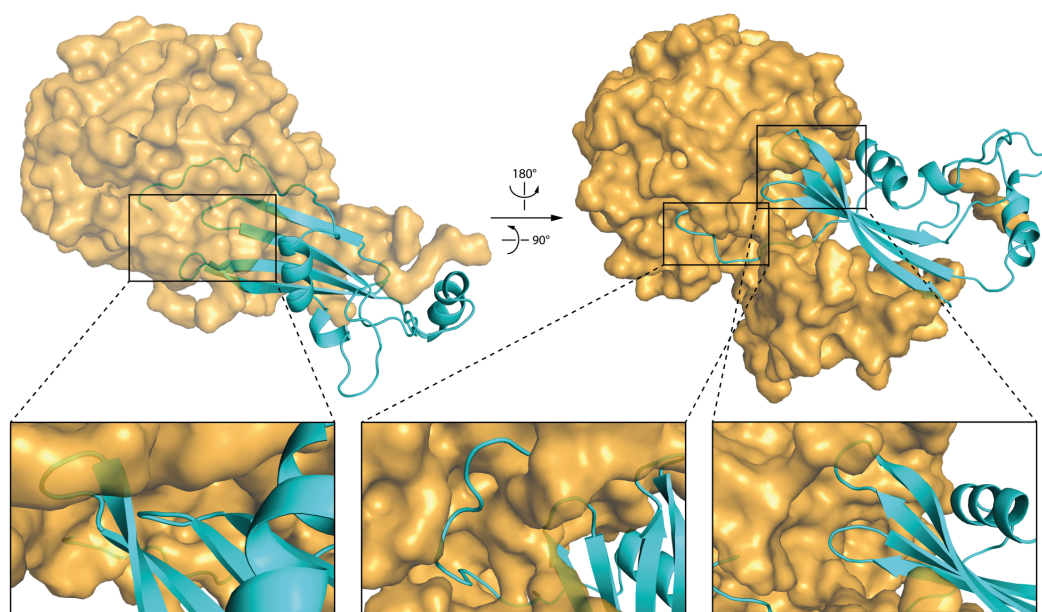


**Figure S6.** The structure of *hCC* WT (*hCC*-2) and DPC:SDS micelle complex after the MD simulations; insets present magnified fragments of the complex.

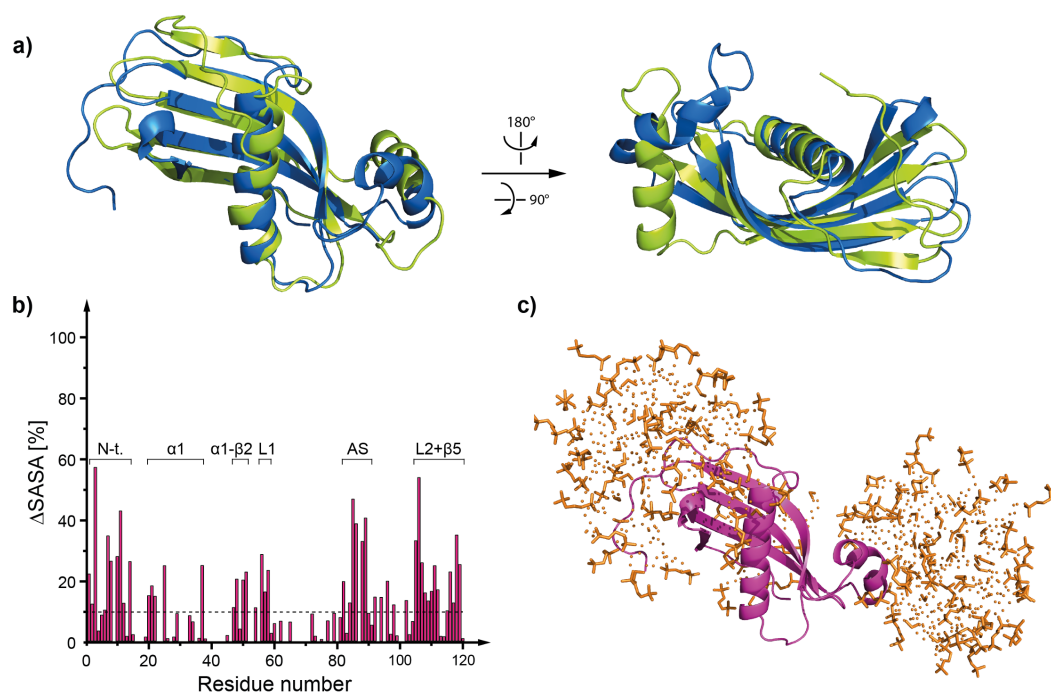


**Figure S7.** (a) The structure of *hCC* WT (hCC-3) monomer before (green) and after (blue) 80 ns of MD simulation of *hCC*-DPC:SDS mixed micelle interaction; (b) histogram visualizing the percentage of the decrease of solvent accessible surface occurring as a consequence of the interaction between *hCC* V57G monomer and DPC:SDS mixed micelle; (c) a model of *hCC* V57G monomer protein interacting with the DPC:SDS mixed micelle, corresponding to the histogram (structure after 80 ns of MD); ΔSAS calculated as a difference between the SAS for the protein model without the micelle and protein model surrounded by the micelle.

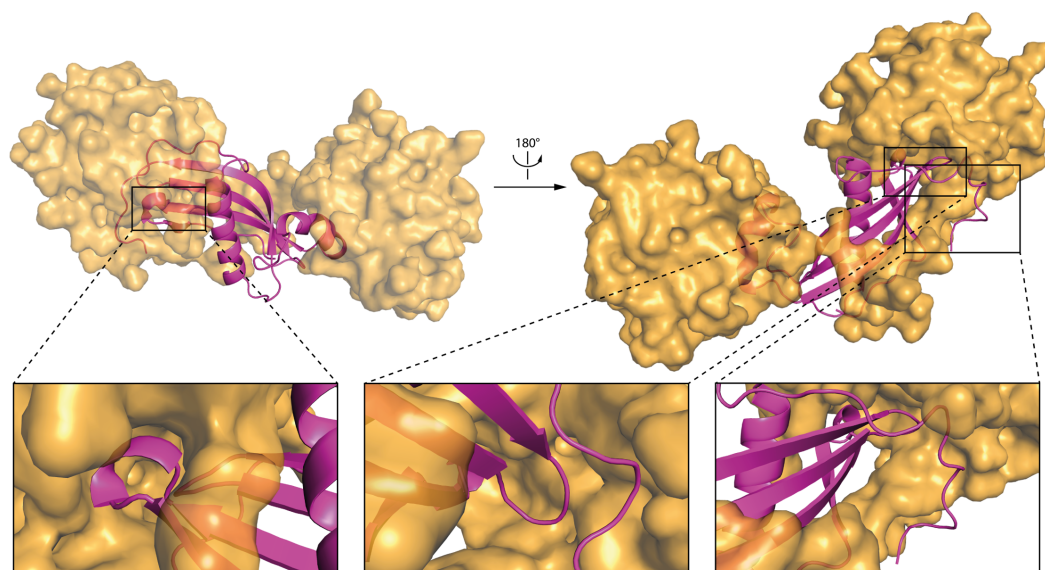


**Figure S8.** The structure of *hCC* WT (*hCC*-3) and DPC:SDS micelle complex after the MD simulations; insets present magnified fragments of the complex.

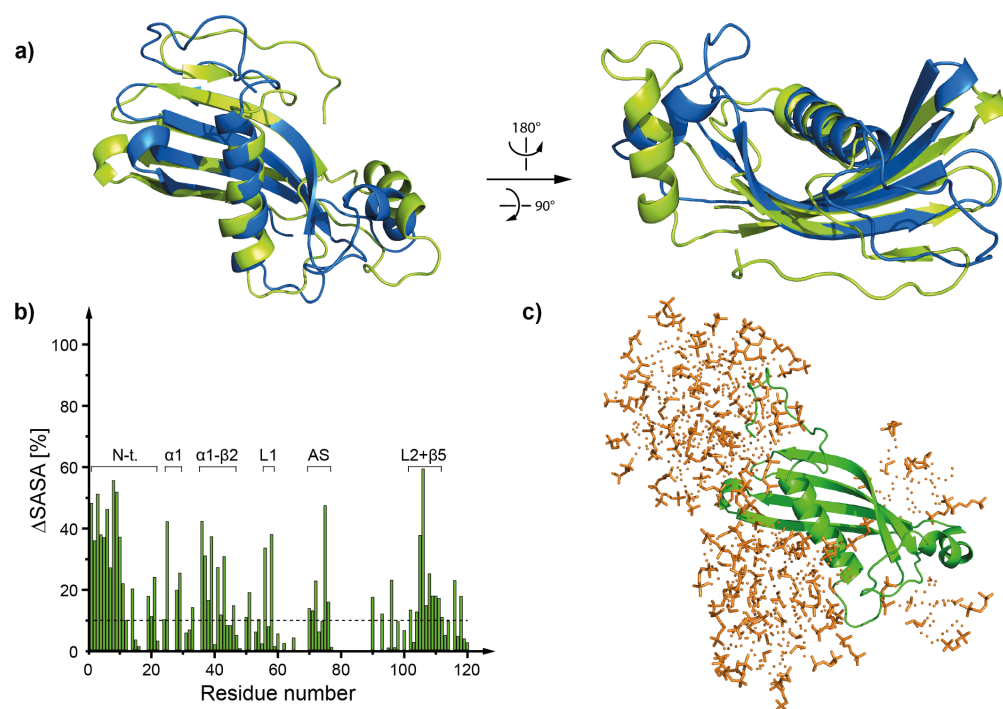


**Figure S9.** (a) The structure of *hCC* V57G (V57G-1) monomer before (green) and after (blue) 80 ns of MD simulation of *hCC*-DPC:SDS mixed micelle interaction; (b) histogram visualizing the percentage of the decrease of solvent accessible surface occurring as a consequence of the interaction between *hCC* V57G monomer and DPC:SDS mixed micelle; (c) a model of *hCC* V57G monomer protein interacting with the DPC:SDS mixed micelle, corresponding to the histogram (structure after 80 ns of MD);  $\Delta$ SAS calculated as a difference between the SAS for the protein model without the micelle and protein model surrounded by the micelle.

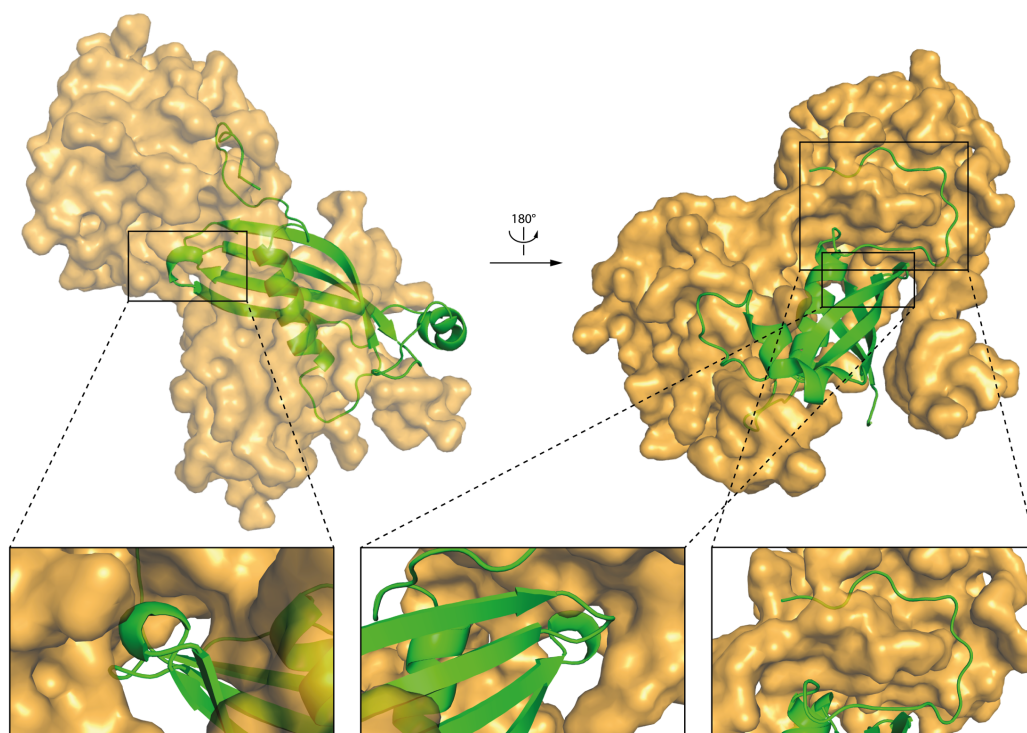


**Figure S10.** The structure of *hCC* V57G (V57G-1) and DPC:SDS micelle complex after the MD simulations; insets present magnified fragments of the complex.

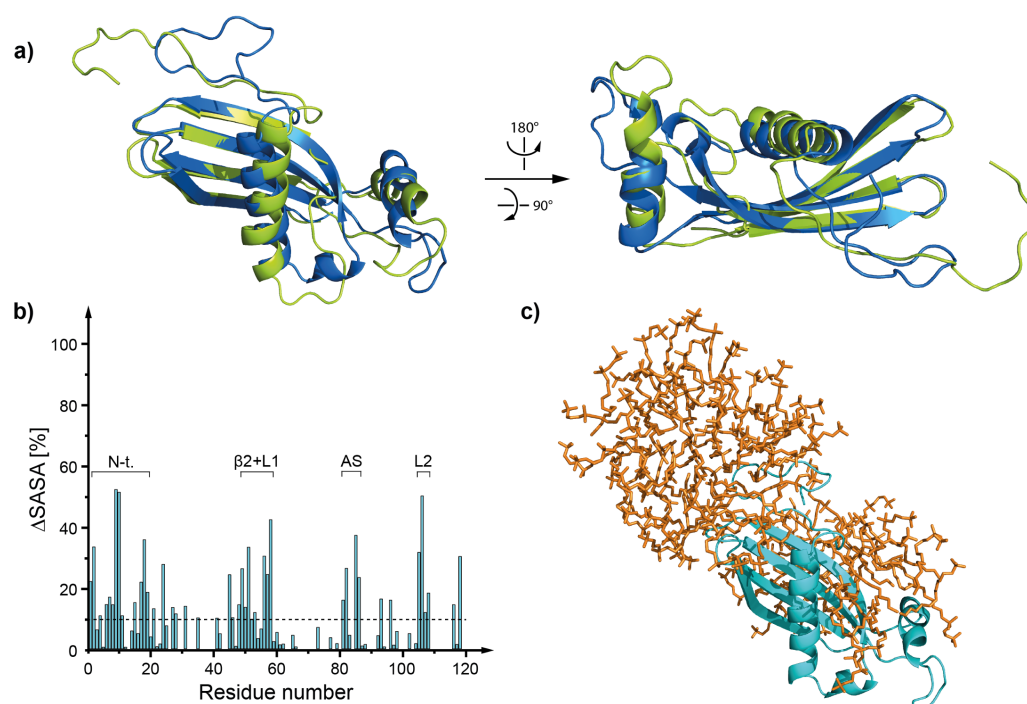


**Figure S11.** (a) The structure of *hCC* V57G (V57G-2) monomer before (green) and after (blue) 80 ns of MD simulation of *hCC*-DPC:SDS mixed micelle interaction; (b) histogram visualizing the percentage of the decrease of solvent accessible surface occurring as a consequence of the interaction between *hCC* V57G monomer and DPC:SDS mixed micelle; (c) a model of *hCC* V57G monomer protein interacting with the DPC:SDS mixed micelle, corresponding to the histogram (structure after 80 ns of MD);  $\Delta$ SAS calculated as a difference between the SAS for the protein model without the micelle and protein model surrounded by the micelle.

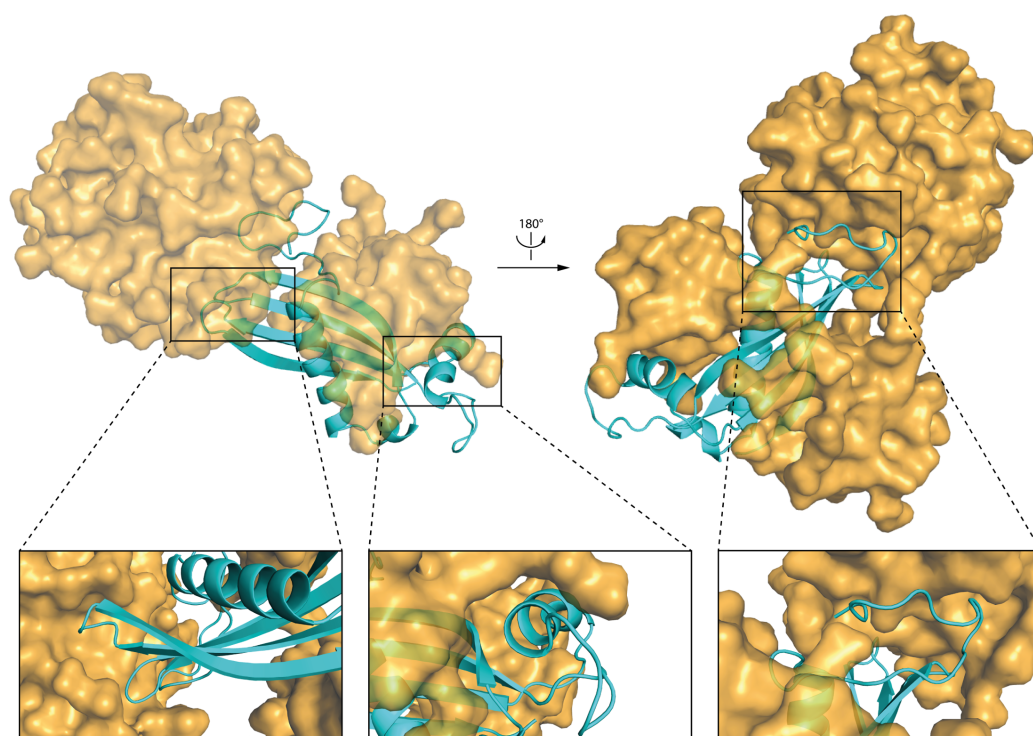


**Figure S12.** The structure of *hCC* V57G (V57G-2) and DPC:SDS micelle complex after the MD simulations; insets present magnified fragments of the complex.

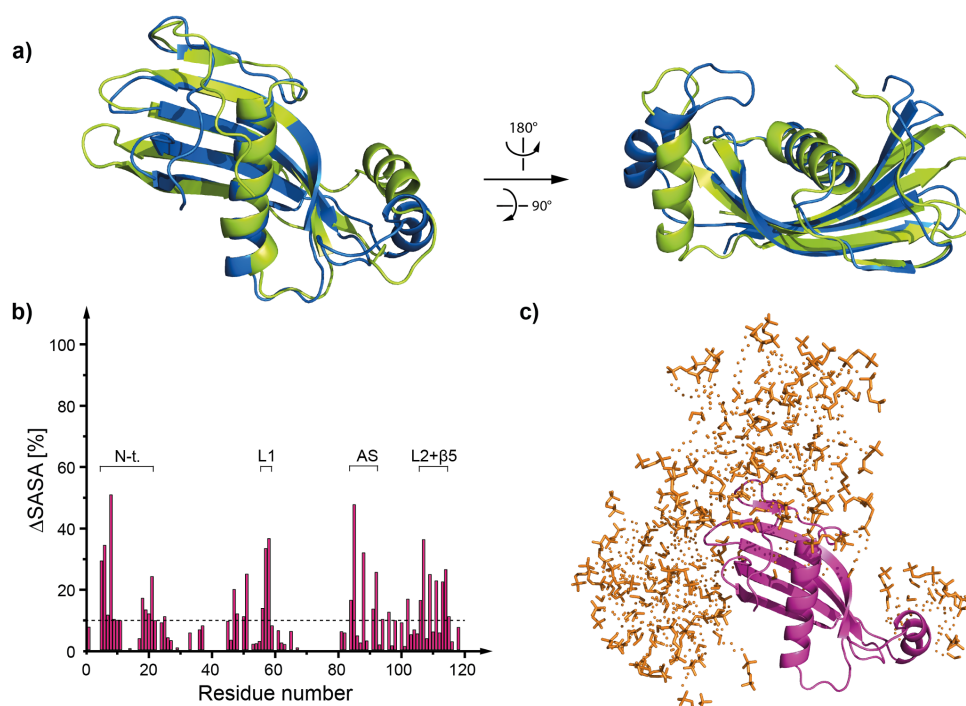


**Figure S13.** (a) The structure of *hCC* V57G (V57G-3) monomer before (green) and after (blue) 80 ns of MD simulation of *hCC*-DPC:SDS mixed micelle interaction; (b) histogram visualizing the percentage of the decrease of solvent accessible surface occurring as a consequence of the interaction between *hCC* V57G monomer and DPC:SDS mixed micelle; (c) a model of *hCC* V57G monomer protein interacting with the DPC:SDS mixed micelle, corresponding to the histogram (structure after 80 ns of MD);  $\Delta$ SAS calculated as a difference between the SAS for the protein model without the micelle and protein model surrounded by the micelle.

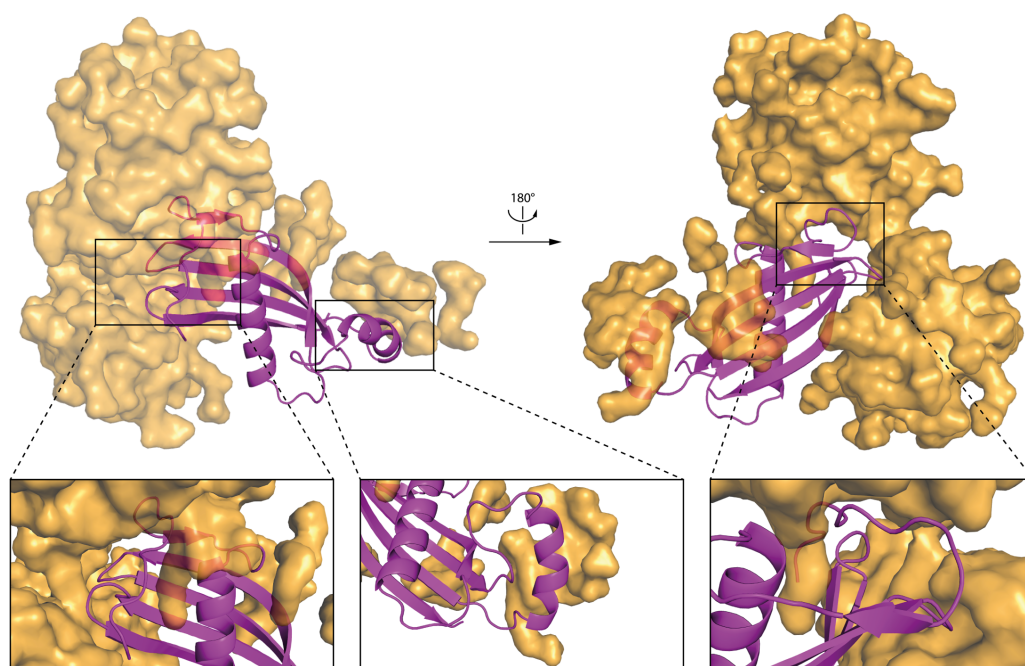


**Figure S14.** The structure of *hCC* V57G (V57G-3) and DPC:SDS micelle complex after the MD simulations; insets present magnified fragments of the complex.

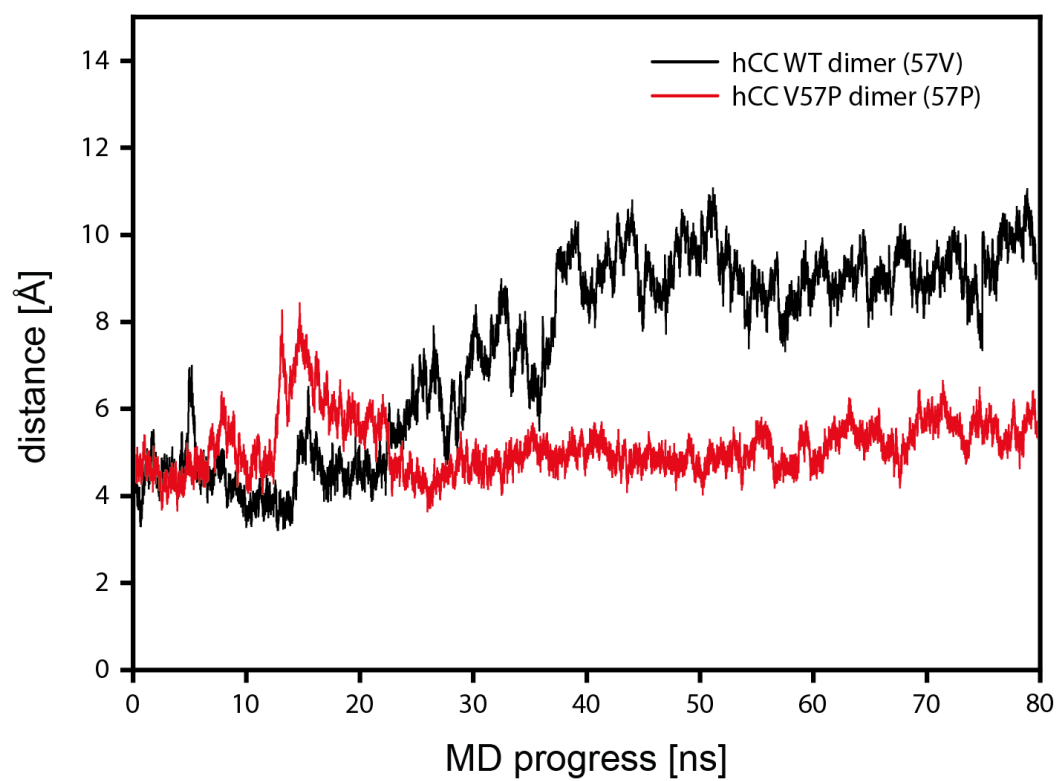


**Figure S15.** Changes in the distance between mass centers of domains in the *hCC* dimers during MD simulations; the comparison for *hCC* WT and *hCC* V57P dimers.

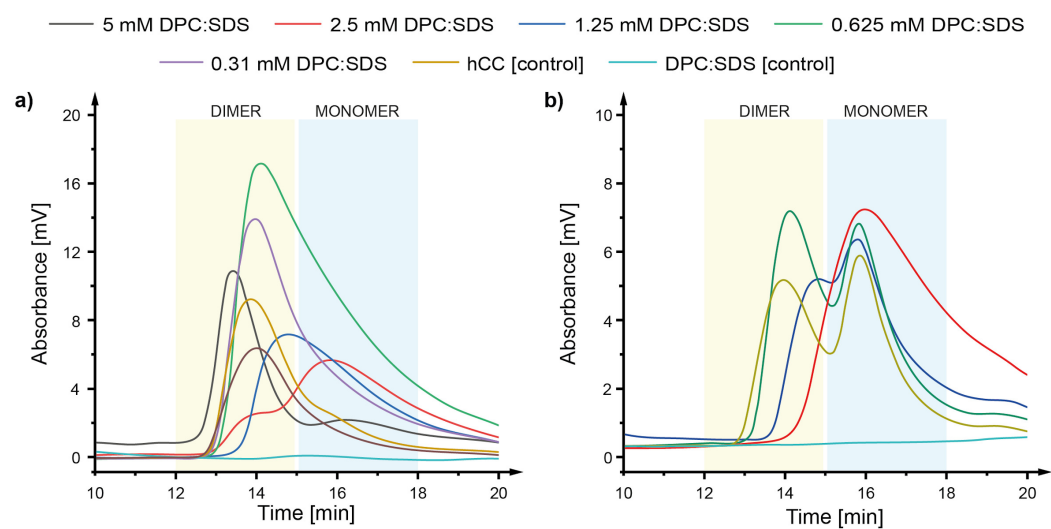


**Figure S16.** Chromatograms visualizing the oligomerization state of (a) *hCC* WT dimer and (b) a mixture of *hCC* WT monomer:dimer (1:1 molar ratio), using the gel filtration chromatography after incubation at 22°C for 24 h in the DPC:SDS (5:1) mixed micelle solution; *hCC* V57P was used as a dimer marker in (a); dimer retention time – ca. 13.5 min (yellow box), monomer retention time – ca. 16 min (blue box).

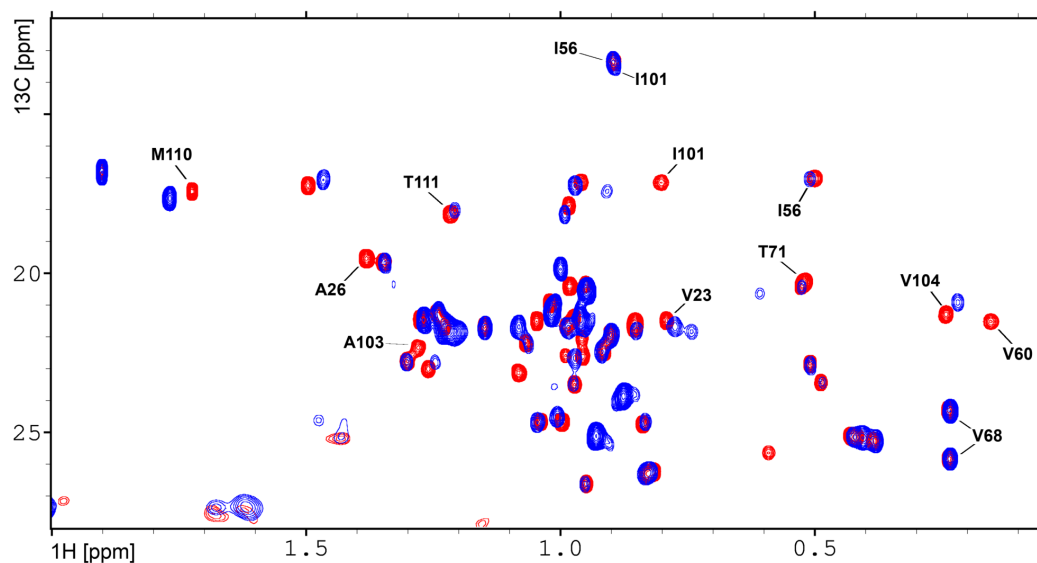


**Figure S17.** Overlay of 2D  $^1\text{H}$ - $^{13}\text{C}$  HSQC spectra (fragment) presenting signals from methyl groups recorded for *hCC V57G* protein only (red) and in the presence of the DPC- $d_{38}$ :SDS- $d_{25}$  micelle (blue). The changes in the position of cross peaks detected for a couple of residues. The increased linewidth in  $^1\text{H}$  dimension observed for some signals resulting from the interaction with the DPC- $d_{38}$ :SDS- $d_{25}$  micelle corresponds to the increased molecular mass.